

---

**APST**

---

**Asia-Pacific Journal of Science and Technology**<https://www.tci-thaijo.org/index.php/APST/index>Published by the Research Department,  
Khon Kaen University, Thailand

---

**Investigation of nanofluid molten salts in a thermocline tank as a thermal energy storage system**Direk Nualsing<sup>1</sup>, Nattadon Pannucharoenwong<sup>1,\*</sup>, Snunkhaem Echaroj<sup>1,\*</sup>, Keyoon Duanguppama<sup>2</sup> and Phadungsak Rattanadecho<sup>1</sup><sup>1</sup> Department of Mechanical Engineering, Faculty of Engineering, Thammasat School of Engineering, Thammasat University, Pathumthani, Thailand<sup>2</sup> Department of Mechanical Engineering, Faculty of Engineering and Industrial Technology, Kalasin University, Kalasin, Thailand

\*Corresponding author: snunkha@engr.tu.ac.th, pnattado@engr.tu.ac.th

Received 4 September 2023

Revised 16 November 2023

Accepted 21 November 2023

---

**Abstract**

Nanoparticles were prepared and incorporated into molten salts to form a nanofluid system for use in a concentrated solar powerplant (CSP). Particle sizes of both the nanoparticles and incorporated molten salts were analyzed from images captured by scanning electron microscopy using image processing software. The heat transfer fluid was prepared via a two-step method by blending four molten salts ( $\text{KNO}_3$ ,  $\text{NaNO}_3$ ,  $\text{LiNO}_3$ , and  $\text{Ca}(\text{NO}_3)_2 \cdot 4\text{H}_2\text{O}$ ) and anodic aluminum oxide (AAO) at  $180^\circ\text{C}$  for 360 minutes. Results showed that after the anodization process, aluminum A5052 transformed the film surface into metal oxide (anodic aluminum oxide) with particle size smaller than 56.3 nm. Incorporation of aluminum nanoparticles into the molten salt matrix increased particle size to 100 nm due to the chemisorption of molten salt by hydroxide functional groups on the AAO surface during the heat transfer process. Addition of AAO improved the discharge power provided by the upright thermocline tank.

**Keywords:** Quaternary molten salts, Nanoparticle, Nanofluid, CSP, Thermal efficiency

---

**1. Introduction**

Nanotechnology is now used in industry, resulting in enormous benefits in material property development and energy conservation, with increased insulation, cooling, energy storage, and reflectivity. Data collected in the United States suggested that 41% of energy is used in residential buildings and offices, with most lost to heat, lighting, and air conditioning [1]. Energy consumption can be greatly reduced by adopting nanotechnology. Nanoparticles are now applied in various fields such as the construction industry [2], medicine [3], food products [4], cosmetics [5], the military, and as catalysts [6]. Nanofluids are suspended solids consisting of metallic or non-metallic particles, with size less than 100 nm, mixed with a liquid, and having a higher thermal conductivity than that liquid, such as copper nanoparticles mixed with water and ethylene [7]. Nanofluids are used in various industries including energy supply and emerging industries in the field of solar systems. Solar harnessing activities utilize nanofluids to increase heat transfer efficiency between the solar collector and the storage tank, which then transforms heat into electricity. Concentrated solar powerplant (CSP) technology converts sunlight or radiated radiation as heat into heat transfer fluid that then delivers the heat into a heat exchanger which produces steam and generates electricity from turning turbines. This technology has the advantage of being able to generate electricity at times of no sunlight, using a heat transfer agent with low power loss.

Molten salt can be used for storing energy from sunlight in the form of a dynamic liquid or a working fluid consisting of at least two types of salts. Current technology mixes  $\text{NaNO}_3$  and  $\text{KNO}_3$  as starting salts, with other ingredients added as thermal materials to improve the thermodynamic properties [8]. Molten salt is commonly used as a eutectic mixture of 60% sodium nitrate and 40% potassium nitrate. This mixture can be heated and liquefied between  $260^\circ\text{C}$  and  $550^\circ\text{C}$ , has a heat of fusion of 161 Joules per gram (J/g), and a heat capacity of 1.53

J/g Kelvin (J/g K) [9]. Molten salt combinations are usually employed as thermal energy storage (TES) systems, with a heating or cooling medium such as water to receive or transfer heat. Many factors affect the amount of energy that can be transferred using heat transfer fluid including the operation duration, the flow rate of the working fluid, outdoor exposure, and the circulation time of the working fluid in CSPs [10-12]. Currently, heat transfer fluids used for CSPs are limited by their high melting temperature and thermal stability. Binary and ternary salt mixtures show potential as effective heat transfer fluids [13,14]. The normalized price of energy (NPOE) must be reduced in CSPs to improve the effectiveness of employing thermal storage system materials such as molten salts. Nanoparticles have recently attracted increased attention as fillers for the development of molten salt nanofluids giving higher thermal conductivity. Nanofluids with added nanoparticles demonstrated high specific heat capacity, constant decomposition temperature, and a slight incline in viscosity compared to other base fluids [15]. New additives and mixtures for photovoltaic power plants as salt blends consisting of  $\text{Ca}(\text{NO}_3)_2$ ,  $\text{KNO}_3$ , and  $\text{NaNO}_3$  were not recommended due to their high viscosity [16], which prevented proper fluid flow throughout the power plant. A mixture containing  $\text{KNO}_3$ ,  $\text{NaNO}_3$ , and  $\text{LiNO}_3$  has a low melting point of 127°C, and it is important to control the  $\text{NaNO}_3$  content as this is responsible for the viscosity of the mixture. Another proposed mixture consisted of  $\text{KNO}_3$  (60%),  $\text{LiNO}_3$  (22%), and  $\text{Ca}(\text{NO}_3)_2$  (18%) with a melting point of 112°C and an appropriate viscosity [17].

The thermodynamic properties are an important aspect of heat exchange systems, and choosing a good heat conductor for heat exchange is very important. Media used in heat exchange include water, ethylene glycol, and oil but these liquids have low thermal conductivity. Therefore, they must be developed to provide better heat conduction efficiency. Nowadays, a popular way to improve thermal conductivity is by adding dispersed solid particles to the medium liquid, known as nanofluid. These solid particles increase the surface area of the heat exchanger and increase the heat capacity of the system, resulting in increased heat conduction efficiency without the need to modify existing equipment [18] In this study, aluminum nanoparticles were mixed with molten salts as a medium to increase thermal efficiency in CSP systems. The novelty of this research lies in the usage of a lithium-based salt and anodic aluminum oxide as the heat transfer agent, which to the best of our knowledge have not been extensively studied.

This research examined the effects of nanoparticles on the thermal properties of quaternary salts for application in CSPs. The thermal energy storage system comprised the four nitrate salts  $\text{NaNO}_3$ ,  $\text{KNO}_3$ ,  $\text{LiNO}_3$ , and  $\text{Ca}(\text{NO}_3)_2 \cdot 4\text{H}_2\text{O}$ . The additive used was aluminum foil that had been exposed to anodization to create a porous surface film. The selected starting salts were mixed with the nano aluminum composite (A5052-H32), and the physical properties were measured by Field Emission Scanning Electron Microscope (FE-SEM). The discharge power of molten salts with different concentrations of additive and molten salt flow rate were used to benchmark different operational scenarios.

## 2. Materials and methods

Aluminum foil (A5052-H32) with thickness 0.5 mm and area 3x3 cm was cleansed in NaOH solution, submerged in 50% isopropanol and dried in nitrogen gas for 24 hours. Anodization of the aluminum foil representing the anode electrode was conducted in concentrated sulfuric acid (2M) with a solid platinum cathode. The anodization process was performed at 120V, 10°C for 30 minutes. Before the anodization process, the anodized aluminum oxide film was submerged in phosphoric acid solution (20 wt%) and then cleansed at 35°C in an ultrasound bath for 10 minutes. Sandpaper was used to polish the surface of the anodized aluminum sheet to give about 2 g of nanoparticles, resulting in an aluminum plate shown in Figure 2(A).

A two-step drying method involved grinding the nanoparticles and molten salt mixture. The other molten salts were combined with  $\text{KNO}_3$  and  $\text{NaNO}_3$  at a weight ratio of 51:49. The combination was melted for 6 hours at 360°C, then cooled to 25°C, and ground to turn the solid eutectic salt mixture into a uniform powder. The  $\text{Al}_2\text{O}_3$  (1 wt%) nanomaterial was then added and the mixture was placed in an aluminum flask to reduce the moisture content before analysis [16], with results shown in Table 1. The compositions of the nanofluid mixtures including anodized aluminum oxide (AAO) are presented in Table 2.

**Table 1** Preparation and characterization methodology

Process	Method	Characterization
1. Preparation of A5052 aluminum	Anodized one sample at thickness of 5, 10, 15 micrometers	The surface basic structure was examined by scanning electron microscopy (SEM)
2. Sheet, size 5x5 cm, 3 samples each	Surface etching	Nanoparticles smaller than 100 nm
3. Preparation of quaternary nitrate salt	Two-step drying technique	Quaternary nitrate salt (basic salt)
4. Preparation of nanofluid	Heating the quaternary nitrate salt (basic salt) at 120 °C for 10 hours and adding nanoparticles	Nanofluid

**Table 2** Compositions of nanofluid mixtures including anodized aluminum oxide (AAO)

Composite		KNO <sub>3</sub>	NaNO <sub>3</sub>	LiNO <sub>3</sub>	Ca(NO <sub>3</sub> ) <sub>2</sub> ·4H <sub>2</sub> O	AAO
Mole molecule		101.10	85.00	68.40	236.00	26.98
Salt ratio (wt%)	A	19.54	16.43	15.72	48.11	0.20
	B	19.54	16.43	15.67	48.06	0.30
	C	19.54	16.43	15.62	48.01	0.40
	D	19.54	16.43	15.57	47.96	0.50

### 3. Results and discussion

Anodization of the aluminum foil was accomplished in a concentrated acid solution using lead as the cathode and surfactant mixtures to facilitate the pore opening mechanism. The anodized foil morphology is shown in Figure 1. The physical characteristics of the aluminum foil were slightly altered and less reflective after the anodization process, indicating a change in the surface texture. This was anticipated because the anodization process caused the surface to lose electrons, turning the metal structure into aluminum oxide [19,20]. With hydroxide surfaces, the anodic aluminum oxide represented a heterogeneous site for the chemisorption of molten salt during the heat transfer process [21,22]. The SEM image of the anodic aluminum oxide is illustrated in Figure 1(B). The granular structure with uniform size is clearly shown, indicating loss of electrons and formation of a hydroxide surface. The uniform grain size suggested adequate mixing during anodization and the absence of a dead zone inside the anodization vessel.

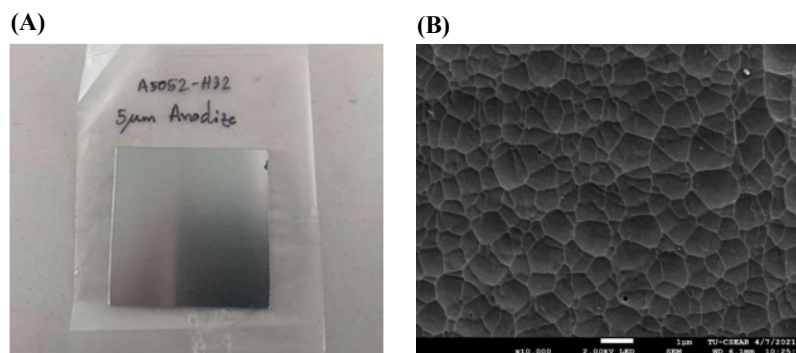


**Figure 1** (A) Aluminum foil 15 µm A5052-H32 and (B) SEM image of anodized aluminum foil under 10,000x magnification.

AAO nanoparticles were prepared using sandpaper. After physical treatment, the AAO nanoparticles were collected and subjected to SEM analysis, as shown in Figure 2 to determine average particle size as 56 nm.

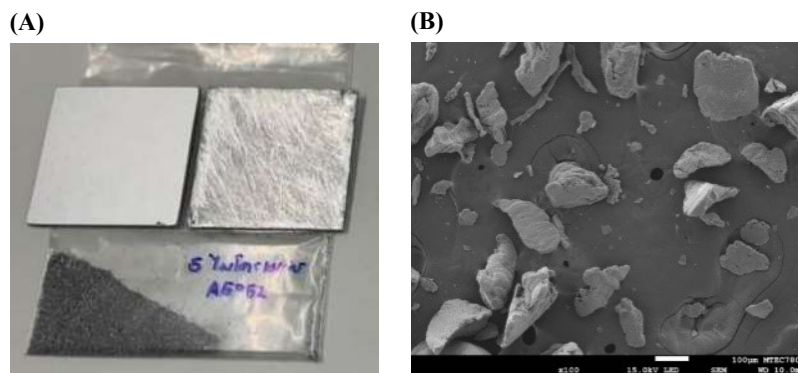


**Figure 2** (A) Anodized aluminum foil after treatment, and (B) SEM image of nanoparticles produced from physical treatment of anodized aluminum foil under 100x magnification.

The AAO nanoparticles were added to mixtures of the molten salts at different compositions. SEM images of anodic aluminum oxide incorporated in the molten salt mixture are shown in Figure 3. According to the image processing software, the average particle size was 100 nm. An increase in the size of incorporated AAO nanoparticles was consistent with other research [23]. Agglomeration of molten salt ions on AAO was due to the hydroxyl group on the surface of AAO [24]. Reinforcement of the AAO nanoparticles improved the thermal conductivity of the molten salt solution, especially in a rigid form.

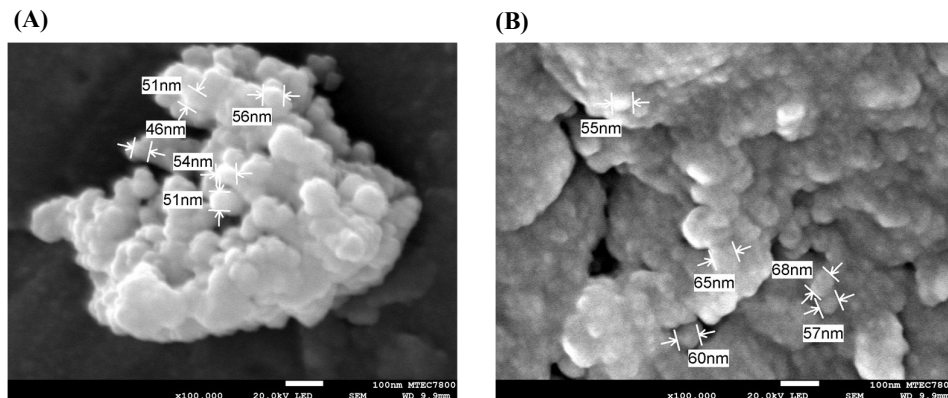


**Figure 3** SEM images of (A) agglomerated nanofluid, and (B) the surface of incorporated AAO under 100,000x magnification.

Performance testing of the molten salt system with different concentrations of AAO additive was conducted in a stainless-steel thermocline tank with different types of filler material, as shown in Figure 4. Stainless steel balls provided the highest discharge power of 8.5 MW at a molten salt flow rate of 0.3 m<sup>3</sup>/h. An increase in the flow rate of the molten salt resulted in a gradual increase in discharge power. The other filler materials provided discharge power ranging between 6.0 and 7.9 MW, and significantly lower than the stainless steel balls. The superior thermal conductivity of the stainless steel balls facilitated heat transfer of the filler material to the molten salts during discharge and from molten salts to the filler material during the charging cycle [25,26]. The filler material that provided the highest discharge power was used to test the performance of molten salts with different amounts of additives.

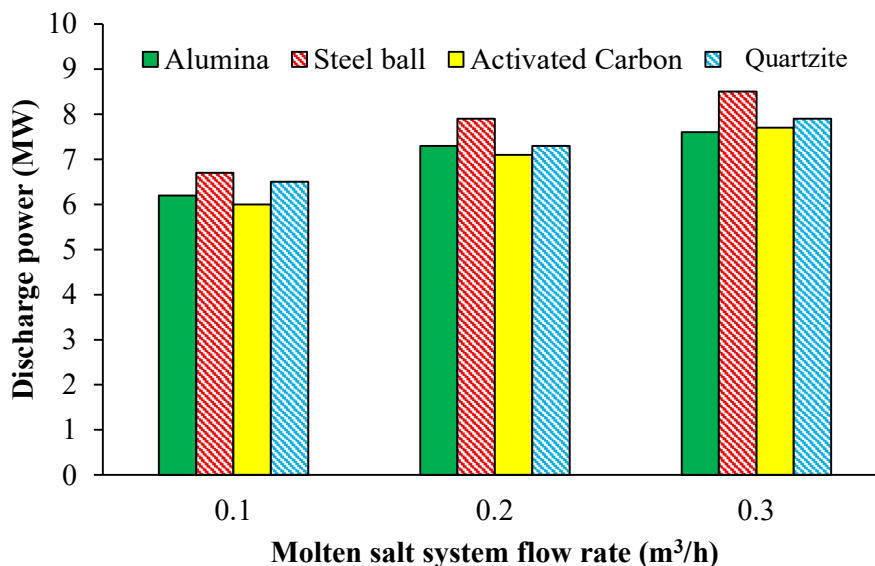


**Figure 4** Discharge power of the thermocline tank at different molten salt flow rates and types of filler material as heat transfer receiver, with the molten salts containing 2.5% AAO additives.

Stainless stain balls were used in the thermocline tank to conduct performance testing of the molten salts with different contents of AAO additives. An increase in AAO from 1.5% to 2.5% significantly increased the discharge

power by 19.6% from 5.6 MW to 6.7 MW. However, as the amount of AAO additive increased to 3.5% and 4.5%, the discharge power did not significantly increase. The highest change in discharge power of 27.4% was observed as the flow rate changed from 0.1 to 0.2 m<sup>3</sup>/h, as shown in Figure 5 and Figure 6. A further increase in flow rate from 0.2 to 0.3 m<sup>3</sup>/h resulted in a reduction in the percentage increase of discharge power because at higher flow velocity some of the ceramic ball fillers broke, resulting in the loss of heat transfer capability.

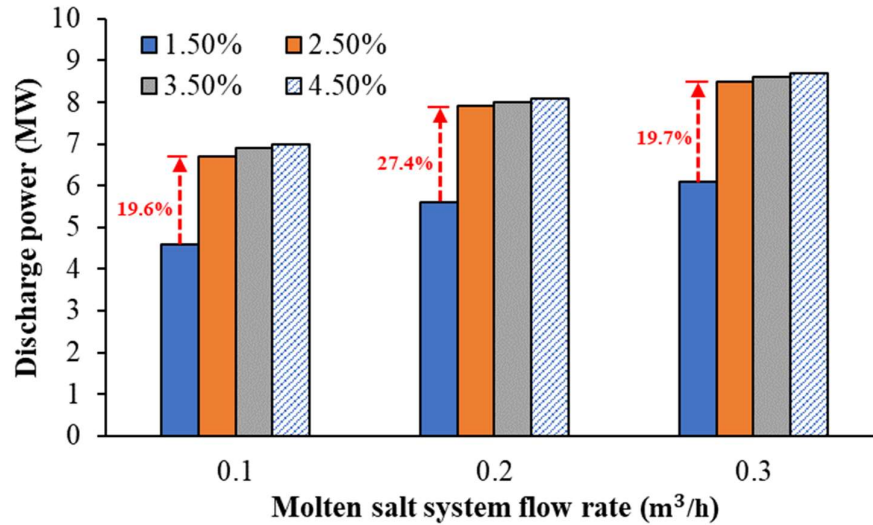


**Figure 5** Discharge power of the thermocline tank at different molten salt flow rates and amounts of AAO additives using stainless steel balls as the filler material.

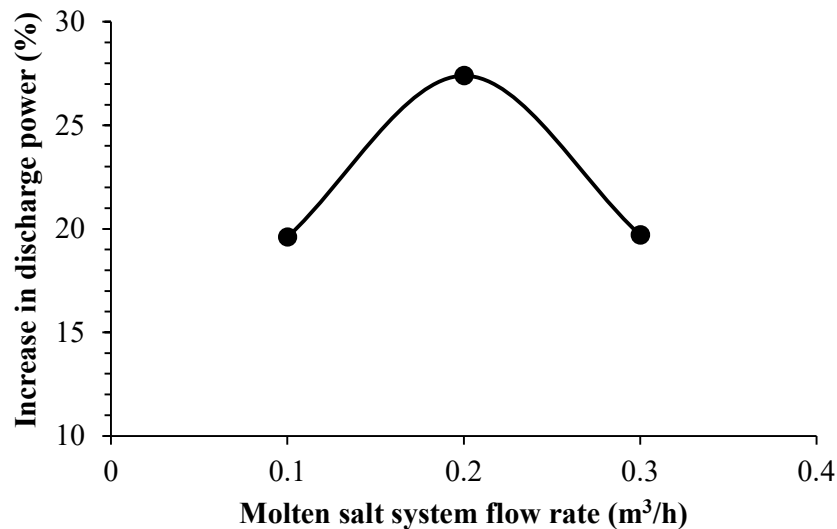


**Figure 6** Percentage increase in discharge power at different flow rates as the concentration of heat transfer agent increased from 1.5% to 2.5%.

#### 4. Conclusions

This research addressed heat transfer efficiency problems in the charging and discharging activities of a thermocline tank. Different alternatives were studied including alteration of the heat transfer agent concentration and the flow rate of the molten salt system. Nanoparticles were prepared by anodizing the aluminum foil before combining with molten salts to form the nanofluid used as a thermal energy storage medium inside a thermocline tank. SEM images of AAO nanoparticles suggested an average particle size of 56 nm. After the incorporation of AAO in the molten salts, particle size increased to 100 nm, indicating significant agglomeration of the molten

salts on the AAO surface. Discharge power peaked when stainless steel balls were used as the filler material inside the thermocline tank. The highest discharge power achieved for stainless steel balls was 8.5 MW, conducted at 0.3 m<sup>3</sup>/h flow rate with 3.5 wt% additive. Our results can be used to design a heat transfer facility of an actual CSP using the novel molten salt system investigated at different flow rates and heat transfer agent concentrations.

## 5. Acknowledgements

This research was funded by Thammasat School of Engineering (TSE), Thammasat University. It was also supported by Mechanical Department and the Thailand Science Research and Innovation Fundamental Fund fiscal year 2023 (Contract No. TUFF180228/2566) and (TUFF41/2566) and this study was supported by Thammasat University Research Fund (Contract No. TUFT 35/2567) and special thanks to National Research Council of Thailand (NRCT) (Contact no. N42A650197).

## 6. References

- [1] Alvarado R, Ortiz C, Ponce P, Toledo E. Chapter 12 - Renewable energy consumption, human capital index, and economic complexity in 16 Latin American countries: evidence using threshold regressions. In: Shahbaz M, Tiwari AK, Sinha A, editors. *Energy-Growth Nexus in an Era of Globalization*: Elsevier; 2022. p. 287-310.
- [2] Barbhuiya S, Das BB. Life Cycle Assessment of construction materials: Methodologies, applications and future directions for sustainable decision-making. *Case Studies Const Mater* 2023;19:02326.
- [3] Xie K, Zhu S, Gui P, Chen Y. Coordinating an emergency medical material supply chain with CVaR under the pandemic considering corporate social responsibility. *Comp Ind Engin* 2023;176:108989.
- [4] Haris M, Hussain T, Mohamed HI, Khan A, Ansari MS, Tauseef A, et al. Nanotechnology – A new frontier of nano-farming in agricultural and food production and its development. *Sci Tot Envir* 2023;857:159639.
- [5] Dubey SK, Dey A, Singhvi G, PandeyMM, Singh V, Kesharwani P. Emerging trends of nanotechnology in advanced cosmetics. *Coll Surf B: Biointer.* 2022;214:112440.
- [6] Sheikh ZUD, Bajar S, Devi A, Rose PK, Suhag M, Yadav A, et al. Nanotechnology based technological development in biofuel production: current status and future prospects. *Enzy Micro Tech.* 2023;171:110304.
- [7] Ravi S, Arun Balasubramanian K, Nagaraj G, Kailasanathan C. Investigations on thermo-physical properties of ethylene glycol-based hybrid Al<sub>2</sub>O<sub>3</sub> and ZrO<sub>2</sub> nanofluid as coolant. *Mater Tod: Proc.* 2023.
- [8] Zhang H, Wang K, Yu W, Wang L, Xie H. Ternary molten salt energy storage coupled with graphene oxide-TiN nanofluids for direct absorption solar collector. *Ener Build.* 2021;253:111481.
- [9] Ma B, Shin D, Banerjee D. One-step synthesis of molten salt nanofluid for thermal energy storage application – a comprehensive analysis on thermophysical property, corrosion behavior, and economic benefit. *J. Energ Storage.* 2021;35:102278.
- [10] Gong Q, Hanke A, Kessel F, Bonk A, Bauer T, Ding W. Molten chloride salt technology for next-generation CSP plants: Selection of cold tank structural material utilizing corrosion control at 500 °C. *Solar Ener Mater Solar Cells.* 2023;253:112233.
- [11] Giaconia A, Iaquaniello G, Metwally AA, Caputo G, Balog I. Experimental demonstration and analysis of a CSP plant with molten salt heat transfer fluid in parabolic troughs. *Solar Ener.*2020;211:622-632.
- [12] Yao Y, Ding J, Liu S, Wei X, Wang W, Lu J. Thermodynamic assessment of binary chloride salt material for heat transfer and storage applications in CSP system. *Solar Ener Mater Solar Cells.* 2023;256:112333.
- [13] Cui L, Yu Q, Huang C, Zhang Y, Wang Y, Wei G, et al. Nano additives induced enhancement of thermal energy storage properties of molten salt: Insights from experiments and molecular dynamics simulations. *J Ener Stor.* 2023;72:108612.
- [14] Yang X, Ji C, Liu J, Ma Y, Cao B. New insights into the heat capacity enhancement of nano-SiO<sub>2</sub> doped alkali metal chloride molten salt for thermal energy storage: A molecular dynamics study. *J Ener Stor.* 2023;63:107015.
- [15] Liu K, Wang N, Pan Y, Alahmadi TA, Alharbi SA, Jhanani GK, et al. Photovoltaic thermal system with phase changing materials and MWCNT nanofluids for high thermal efficiency and hydrogen production. *Fuel.* 2024;355:129457.
- [16] Salehi R, Jahanbakhshi A, Ooi JB, Rohani A, Golzarian MR. Study on the performance of solar cells cooled with heatsink and nanofluid added with aluminum nanoparticle. *Inter J Thermo.* 2023;20:100445.
- [17] Liang F, Wei X, Lu J, Ding J, Liu S. Interplay between interfacial layer and nanoparticle dispersion in molten salt nanofluid: Collective effects on thermophysical property enhancement revealed by molecular dynamics simulations. *Int J Heat Mass Transf.* 2022;196:123305.
- [18] Cui L, Yu Q, Wei G, Du X. Mechanisms for thermal conduction in molten salt-based nanofluid. *Int J Heat Mass Transf.* 2022;188:122648.

- [19] Yu X, Zhang G, Zhang Z, Wang Y. Research on corrosion resistance of anodized and sealed 6061 aluminum alloy in 3.5 % sodium chloride solution. *Inter Jour Electrochem Sci.* 2023;18(5):100092.
- [20] Nualsing D, Pannuchaoenwong N, Echaroj S, Rattanadecho P. Investigation of molten salts incorporated with anodic aluminum oxide as thermal energy storage fluid on heat transfer efficiency. *Case Studies Ther Engin.* 2023;49:103258.
- [21] Choma P, Bazin I, Cerutti M, Vena A, Sorli B. Capacitive immunosensor based on grafted Anodic Aluminum Oxide for the detection of matrix metalloproteinase 9 found in chronic wounds. *Analy Biochem.* 2023;678:115282.
- [22] Eessaa AK, El-Shamy AM. Review on fabrication, characterization, and applications of porous anodic aluminum oxide films with tunable pore sizes for emerging technologies. *Microelect Engin* 2023;279:112061.
- [23] Liu J, Xiao X. Molecular dynamics investigation of thermo-physical properties of molten salt with nanoparticles for solar energy application. *Ener.* 2023;282:128732.
- [24] Xian L, Chen L, Tian H, Tao W-Q. Enhanced thermal energy storage performance of molten salt for the next generation concentrated solar power plants by SiO<sub>2</sub> nanoparticles: A molecular dynamics study. *Appl Ener.* 2022;323:119555.
- [25] Elsihy ES, Liao Z, Xu C, Du X. Dynamic characteristics of solid packed-bed thermocline tank using molten-salt as a heat transfer fluid. *International J Heat Mass Trans.* 2021;165:120677.
- [26] Elsihy ES, Wang X, Xu C, Du X. Numerical investigation on simultaneous charging and discharging process of molten-salt packed-bed thermocline storage tank employing in CSP plants. *Renew. Ener.* 2021;172:1417-1432.